Clin Exp Nephrol (2015) 19:576–584
DOI 10.1007/s10157-014-1032-8

ORIGINAL ARTICLE

Apoptosis induced by an uromodulin mutant C112Y and its suppression by topiroxostat

Sulistiyati Bayu Utami · Endang Mahati · Peili Li · Nani Maharani · Nobuhito Ikeda · Udin Bahrudin · Chishio Munemura · Makoto Hosoyamada · Yasutaka Yamamoto · Akio Yoshida · Yuji Nakayama · Katsumi Higaki · Eiji Nanba · Haruaki Ninomiya · Yasuaki Shirayoshi · Kimiyoshi Ichida · Kazuhiro Yamamoto · Tatsuo Hosoya · Ichiro Hisatome

Received: 4 July 2014 / Accepted: 9 September 2014 / Published online: 20 September 2014

Abstract

Background Familial juvenile hyperuricemic nephropathy (FJHN) is an autosomal dominant disorder caused by mutations in *UMOD* that encodes uromodulin. Topiroxostat, a novel non-purine analog, selectively inhibits xanthine oxidase and reduces the serum uric acid levels and the urinary albuminuria.

Methods Genomic DNA of a patient was extracted from peripheral white blood. Exons and flanking sequences of *UMOD* were amplified by PCR with primers. Mutation analysis was performed by direct sequencing of the PCR products. The wild-type and mutant uromodulin were expressed in HEK293 cells and analyzed by western blotting, immunoprecipitation, immunofluorescence, and flow cytometry.

Results We identified an FJHN patient who carried a novel *UMOD* mutation G335A (C112Y). The levels of both cytosolic and secreted C112Y protein were significantly decreased compared with the wild-type, whereas the level of ubiquitination was higher in C112Y than that in the wild type. The half-life of C112Y was shortened and it was restored by a proteasome inhibitor MG132. Immunofluorescence revealed decreased levels of C112Y in the Golgi apparatus and on the plasma membrane. Expression of C112Y induced cellular apoptosis as revealed by flow cytometry. Apoptosis induced by C112Y was suppressed by topiroxostat.

S. B. Utami and E. Mahati have equally contributed to this manuscript.

Electronic supplementary material The online version of this article (doi:10.1007/s10157-014-1032-8) contains supplementary material, which is available to authorized users.

S. B. Utami · E. Mahati · P. Li (✉) · N. Maharani · N. Ikeda · Y. Yamamoto · A. Yoshida · Y. Shirayoshi · I. Hisatome
Division of Regenerative Medicine and Therapeutics, Department of Genetic Medicine and Regenerative Therapeutics, Institute of Regenerative Medicine and Biofunction, Tottori University Graduate School of Medical Science, 86 Nishichou, Yonago 683-8503, Japan
e-mail: peili-li@med.tottori-u.ac.jp

S. B. Utami · U. Bahrudin
Department of Cardiology and Vascular Medicine, Faculty of Medicine, Diponegoro University, Semarang, Indonesia

C. Munemura
Division of Medicine and Clinical Science, Department of Multidisciplinary Internal Medicine, School of Medicine, Tottori University Faculty of Medicine, Yonago, Japan

M. Hosoyamada
Department of Human Physiology and Pathology, Faculty of Pharma-Sciences, Teikyo University, Tokyo, Japan

Y. Nakayama · K. Higaki · E. Nanba
Division of Functional Genomics, Research Center for Bioscience and Technology, Tottori University, Yonago, Japan

H. Ninomiya
Department of Biological Regulation, Tottori University Faculty of Medicine, Yonago, Japan

K. Ichida
Department of Pathophysiology, Tokyo University of Pharmacy and Life Sciences, Tokyo, Japan

K. Yamamoto
Division of Cardiovascular Medicine, Department of Molecular Medicine and Therapeutics, Tottori University, Yonago, Japan

T. Hosoya
Department of Pathophysiology and Therapy in Chronic Kidney Disease, Jikei University School of Medicine, Minato-ku, Tokyo, Japan

Conclusion C112Y causes its protein instability resulting cellular apoptosis which could be suppressed with topiroxostat.

Keywords FJHN · Uromodulin · Protein instability · Apoptosis · Topiroxostat

Introduction

Uromodulin encoded by *uromodulin* (*UMOD*) gene [1, 2] is the most abundant protein secreted in urine [3]. It is expressed by tubular epithelial cells in the thick ascending limb of the loop of Henle and the early distal convoluted tubule [4, 5]. Uromodulin is targeted mainly at the apical membrane via a glycosylphosphatidylinositol (GPI) anchor, where it is cleaved by a cellular protease to be excreted in urine [4, 5]. Uromodulin suppresses urinary tract infection [6] and stone formation [7]. Uromodulin has immunomodulatory actions as evidenced by its capacity to activate neutrophils and monocytes [8] and to regulate innate and adaptive immunity in Toll-like receptor-4-dependent defense mechanisms [9].

Mutations in UMOD cause familial juvenile hyperuricemic nephropathy (FJHN), an autosomal dominant disorder characterized by gout and hyperuricemia associated with chronic kidney disease [1, 10]. Uromodulin is modified by formation of a large number of intrachain disulfide bonds [11]. Most of the uromodulin mutants with alteration of cysteine residues [1] retain in the ER [12, 13], and their levels in urine are markedly reduced [14]. Uromodulin mutants tends to form aggregates because of cross-linking due to nonnative intrachain disulfide bonds [15], resulting in programmed cell death [11]. Thus, a pathological accumulation of the mutant uromodulin protein is the primary cause of renal damage in FJHN [11].

In the present study, we report a novel uromodulin mutation (C112Y) in a patient with FJHN. We found that C112Y destabilizes the protein, alters expression levels of pro-apoptotic and anti-apoptotic proteins, and causes cellular apoptosis. Apoptosis induced by C112Y could be partially suppressed by topiroxostat, which is an orally active non-purine analog, selective xanthine oxidase (XO) inhibitor developed for treatment of hyperuricemia.

Materials and methods

Patients and identification of uromodulin mutation

This study was approved by the Ethical Committee of Faculty of Medicine (approval number 82/G45), Tottori University, and conformed to the principles outlined in the Declaration of Helsinki. Informed consent for participation in this study was obtained from the patient. Proband and the family members included 7 patients in 4 generations who presented clinical features of FJHN. Genomic DNA was extracted from peripheral white blood cells using a standard phenol–chloroform procedure. Except for exon 1, all exons and flanking sequences of *UMOD* were amplified using PCR primers shown in Supplementary Table 1. Exon 3 was amplified using 2 sets of primers. Mutation analysis was performed by direct sequencing of the PCR products (Abi Prism® 373 DNA Sequencer, Applied Biosystems, Foster City).

Plasmid construction and expression

cDNA encoding the wild-type *UMOD* was ligated into a mammalian expression vector pcDNA3.1 (+) (Invitrogen, Carlsbad, CA, USA) at the *Not*I and *Xba*I site. C112Y mutation was generated by using QuikChange Site-Directed Mutagenesis Kit (Stratagene, La Jolla, CA, USA). HEK293 cells were maintained in Dulbecco's modified Eagle's medium (D-MEM, Wako, Osaka, Japan) supplemented with 10 % fetal bovine serum (Nichirei Biosciences, Tokyo, Japan) and 0.5 % penicillin–streptomycin G (Wako, Osaka, Japan) at 37 °C in a 5 % CO_2 incubator. Cells were transfected with the plasmid using Lipofectamine (Invitrogen, Carlsbad, CA, USA) according to manufacturer's instructions. 48 h after transfection, cells and their supernatant were subjected to assays. Proteasome inhibitors, MG132 (Calbiochem,La Jolla, CA, USA) and lactacystine (Sigma, Saint Louis, MO, USA) were dissolved in DMSO. The final concentration of DMSO in the culture medium was equal to or less than 0.01 % v/v. All the other drugs were dissolved in a buffer.

Western blotting and immunoprecipitation

Conditioned medium was collected at 48 h post-transfection. Cells were scraped into lysis buffer (PBS/1 % NP40, 0.5 % sodium deoxycholate, 0.1 % SDS, 10 μg/ml aprotinin, 10 μg/ml leupeptin, 10 μg/ml pepstain, and 1 mM phenylmethylsulfonyl fluoride), lysed by sonication, and insoluble materials were removed by centrifugation. Protein concentrations were determined with a protein assay kit (Bio-Rad, Hercules, CA, USA). Ten μg of proteins was separated on 7.5 % SDS-PAGE and electrotransferred to a PVDF membrane (Immobilon-P, Millipore, Bedford, MA, USA). Membranes were probed with antibodies against uromodulin (1:1000; Santa Cruz, Santa Cruz, CA, USA), β-actin (1:2000; Calbiochem, La Jolla, CA, USA), ubiquitin (1:1000; MBL, Nagoya, Japan), p53 (1:1000; Santa Cruz, Santa Cruz, CA, USA), Bax (1:1000; Santa Cruz, Santa Cruz, CA, USA), cytochrome *c* (1:500; BD

Biosciences, Franklin Lakes, NJ, USA), Bcl-2 (1:1000; Santa Cruz, Santa Cruz, CA, USA), Bcl-xL (1:1000; Santa Cruz, Santa Cruz, CA, USA) or GFP (1:1000; MBL, Nagoya, Japan) and were developed using an ECL system (Amersham, Piscataway, NJ, USA). Immunoprecipitation was carried out in PBS/1 % Triton X-100, 0.5 % SDS, 0.25 % sodium deoxycholate, 1 mM EDTA, and protease inhibitors for 2 h at 4 °C. Immune complexes were collected with protein G-agarose (GE Healthcare, Uppsala, Sweden) and bound proteins were analyzed by SDS-PAGE followed by immunoblotting. Band intensities were quantified using the Image J software (NIH, US).

Semi-quantitative RT-PCR

Total RNAs of transfected HEK293 cells were extracted using RNeasy Plus Mini Kit (QIAGEN, Valencia, CA, USA) and subjected to RT-PCR (PrimeScript RT-PCR Kit, Takara, Shiga, Japan). RNA samples were treated with DNase1 (Promega, Madison, WI, USA) to eliminate genomic DNA.A primer set (forward: 5′-CCAATGACAT GAAGGTGTCG-′ and reverse: 5′-ACTGACCATTGG CTGTAGGG-3′) was used for amplification of a fragment of *UMOD* with a product size of 323 bp. The cDNA of *GAPDH* was amplified using primers (forward: 5′-CGA GATCCCTCCAAAATCAA-3′ and reverse: 5′-GTCTT CTGGGTGGCAGTGAT-3′). The PCR products were separated on an electrophoresis gel, stained with ethidium bromide, and visualized in a UV transilluminator.

Chase analysis

To analyze degradation kinetics of the wild-type and C112Y mutant proteins, HEK293 cells were seeded in 6-well plates and transfected with either wild-type or C112Y plasmid. Protein extracts were prepared at the indicated time after the addition of cycloheximide (60 μg/ml) and subjected to anti-uromodulin Western blotting. Band intensity was quantified using an NIH image software. The decay rate constant (k) was estimated by fitting first-order decay curves of the form $y = e^{-kt}$, using SigmaPlot (Jandel Scientific, USA). The half-life ($t_{1/2}$) of the protein was calculated using the formula $t_{1/2} = 0.693/k$ [16].

Immunofluorescence

HEK293 cells were seeded on gelatin-coated coverslips and transfected with wild-type or C112Y plasmid together with pDsRed2-ER (Clontech), pDsRed-Monomer-Golgi (Clontech) or pPM-mKeima-Red (BML). 24 h later, they were fixed with 4 % paraformaldehyde/PBS and then permeabilized with 0.5 % Triton X-100. After blocking in 3 % albumin, they were incubated for 1 h at room temperature with anti-uromodulin (1:200; Santa Cruz, Santa Cruz, CA, USA). Bound antibodies were visualized with Alexa Fluor 488-conjugated rabbit secondary antibody (1:2000; Invitrogen, Eugene, OR, USA) and images were obtained using a Bio-Rad MRC 1024 confocal microscope. To quantify uromodulin signals, images were cropped with regard to distribution of each marker protein (pDsRed2-ER, pDsRed-Monomer-Golgi or pPM-mKeima-Red) using Photoshop CS3 software (Adobe Systems, USA). Signal intensities in cropped images were quantified by Image J software (NIH, USA).

Flow cytometry

Transfected HEK293 cells were cultivated for 72 h. Cells harvested by trypsinization were fixed by 70 % ethanol overnight at 4 °C. They were centrifuged, treated with RNase, and stained with propidium iodide. Data were acquired by BD FACSCanto II (BD Biosciences, San Jose, CA, USA) flow cytometer and analyzed using FACSDiva software (BD Biosciences, San Jose, CA, USA). Apoptotic cells were labeled using Annexin V-PE Apoptosis Detection Kit Plus according to the manufacturer's instructions (MBL, Nagoya, Japan).

Statistical analysis

Student's unpaired t test was carried out for difference between two groups, while two-way ANOVA test and Fisher's exact test were carried out for multiple comparisons among groups. All data are derived from three or more experiments and expressed as mean ± SEM. A value of $p < 0.05$ was considered statistically significant. Statistical analysis was made by StatView for windows software version 5 (SAS Institute Inc., Cary, NC, USA).

Results

A novel mutation in *UMOD* of a patient with FJHN

A Japanese FJHN family included seven patients in four generations who had hyperuricemia with or without gout or renal insufficiency (Supplementary Fig. 1A). On 1997, at the age of 25, the proband developed recurrent arthritis with hyperuricemia, and was diagnosed for gout arthritis. Although his serum uric acid level was kept lower than 6 mg/dl by oral administration of benzbromarone (50 mg/day) and allopurinol (100 mg/day), the serum creatinine level gradually increased and at the age of 38, he developed end-stage renal insufficiency. His family pedigree showed an autosomal dominant trait of gout and gouty kidney. As

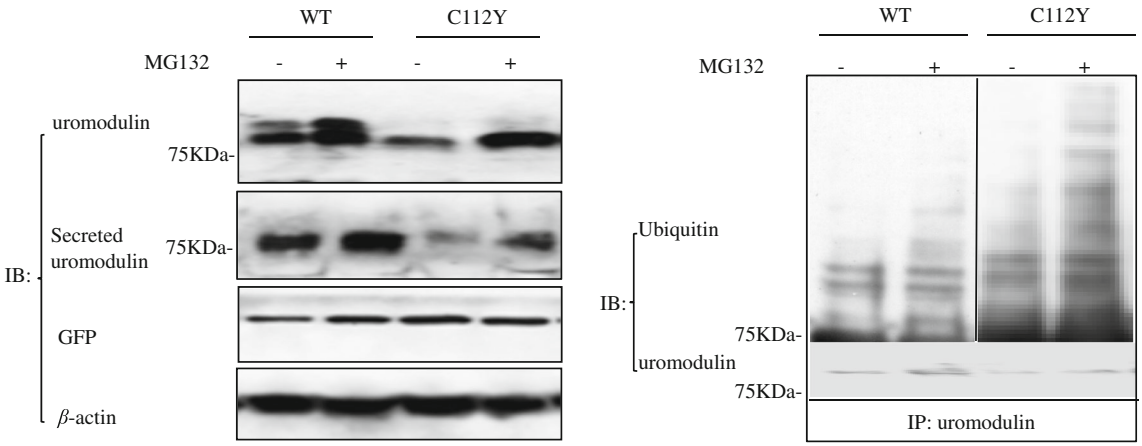

Fig. 1 Protein levels of intracellular and secreted C112Y mutant and its ubiquitination with or without treatment with MG132. *Left panel* Representative immunoblot of WT and C112Y mutant. Cells were transfected with the WT or the C112Y mutant and EGFP plasmid for 48 h, in the absence or presence of MG132 (5 μM, overnight). The condition media were prepared 48 h after the transfection and concentrated. The samples were subjected to immunoblotting (IB) with the indicated antibodies. *Right panel* Effects of MG132 on ubiquitination. Lysates were immunoprecipitated with anti-uromodulin antibody. Anti-uromodulin immunoprecipitates (IP) were subjected to IB with anti-ubiquitin or anti-uromodulin

shown in Supplementary Fig. 1B, in a case of FJHN, analysis of *UMOD* revealed a novel missense mutation C112Y. This mutation is located on exon 3 which encodes the calcium binding motif of an EGF3-like domain.

Proteasomal degradation of the C112Y mutant

The wild-type (WT) uromodulin expressed in HEK293 cells gave two bands on anti-uromodulin Western blotting at ~100 and ~84 kDa which correspond to mature and immature forms, respectively. The level of the mature form of the C112Y mutant was lower than that of the WT, whereas the level of the immature form was comparable with that of the WT (Fig. 1). As expected, the level of the mature C112Y secreted in culture medium was lower than that of the WT (Fig. 1). Both the mutant and WT proteins were recovered in a detergent-soluble fraction, excluding a change in protein solubility (Supplementary Fig. 2). The levels of *UMOD* mRNA were comparable between cells transfected with the WT and those transfected with the C112Y mutant (data not shown). Immunoprecipitation experiments showed a higher level of polyubiquitination of the C112Y mutant. MG132 increased the levels of ubiquitinated protein both in the WT and the C112Y mutant (Fig. 1). The same treatment increased the levels of mature and immature forms of the C112Y mutant (Fig. 1). Uromodulin was recovered in a detergent-soluble fraction regardless of MG132 treatment, excluding MG132-induced change of protein solubility (Supplementary Fig. 2). The secreted protein levels of both C112Y and WT were also increased by MG132 (Fig. 1). Lactacystin, another proteasome inhibitor, had similar effects (Supplementary Fig. 3).

Accelerated degradation of C112Y mutant

To investigate the stability of the C112Y mutant, we determined a half-life of the protein by chase analysis (Fig. 2a–c). Degradation of the immature form of the C112Y mutant was faster with a half-life ($t_{1/2}$) of 3.2 ± 0.02 h than that of the WT with a $t_{1/2}$ of 6.6 ± 0.11 h. MG132 prolonged $t_{1/2}$ of the immature form of the C112Y mutant to 9.6 ± 0.29 h (Fig. 2b, c). These results indicated accelerated degradation of the C112Y mutant through the ubiquitin–proteasome system (UPS).

Next, we examined intracellular distribution of the WT and C112Y mutant in HEK293 cells (Fig. 2d). The immunoreactivity of the WT protein was localized in the endoplasmic reticulum (ER) (nos. 1–3), the Golgi apparatus (nos. 7–9), and the cell membrane (nos. 13–15), as evidenced by co-localization with DsRed2-ER, DsRed-Monomer-Golgi and PM-mKeima-Red, respectively. The signal of C112Y mutant was mainly localized in the ER (nos. 4–6) and was significantly decreased in the Golgi apparatus (nos. 10–12) and on the cell membrane (nos. 16–18). These changes were confirmed by a quantification analysis (Fig. 2e).

Expression of C112Y mutant causes apoptosis

Expression of an unstable mutant protein alters the levels of both pro-apoptotic and anti-apoptotic proteins and causes cellular apoptosis [16]. We examined whether this happens with the C112Y uromodulin. The C112Y mutant increased the levels of pro-apoptotic proteins p53, Bax, and cytochrome *c*, whereas it reduced the levels of anti-apoptotic proteins Bcl-2 and Bcl-xL (Fig. 3a). Flow cytometry

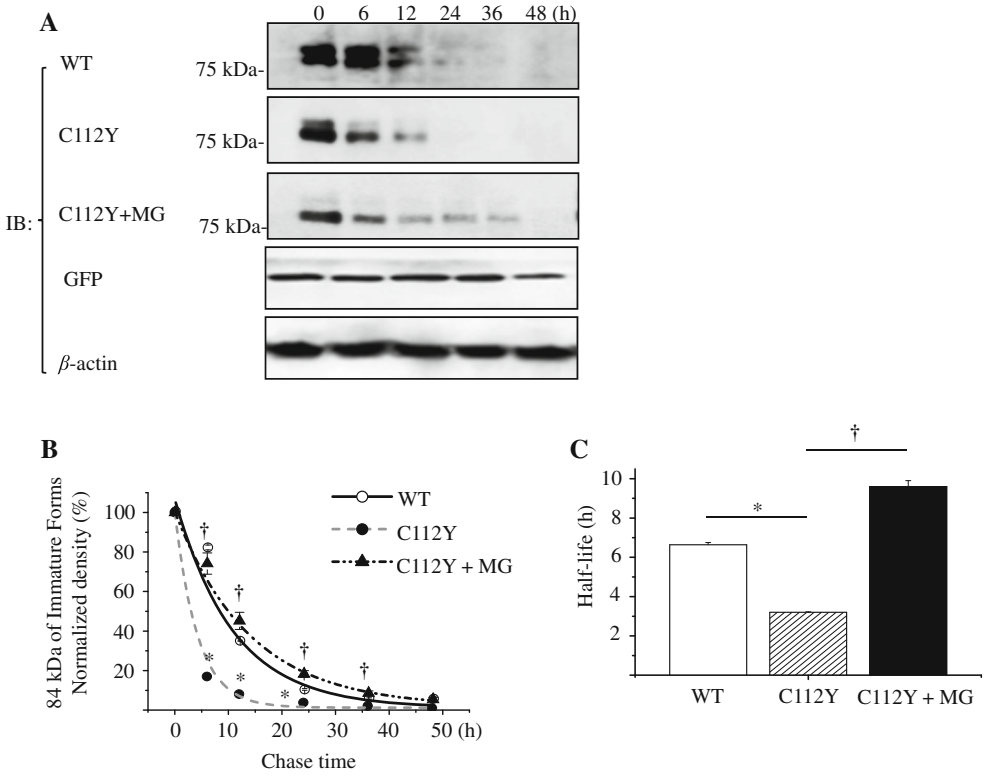

Fig. 2 Accelerated degradation of the C112Y mutant and intracellular localization of the WT and the C112Y mutant. **a** HEK cells transiently expressing the WT or the C112Y mutant were chased for the indicated time after the addition of cycloheximide in the absence and presence of MG132 (5 μM, overnight). Shown are the representative blot and time-dependent changes in the density of the WT and the C112Y mutant. **b** The densities of immature of WT and C112Y uromodulin were normalized to the density at time 0 and β-actin ($n = 3$). $^{*}p < 0.05$. C112Y vs WT, $^{\dagger}p < 0.05$. C112Y vs C112Y + MG. **c** *Bar graph* shows half-life of the WT and the C112Y mutant ($n = 3$). $^{*}p < 0.05$, $^{\dagger}p < 0.05$. **d** Immunofluorescence of the WT and the C112Y mutant expressed in HEK293 cells. Cells were cotransfected with the WT or the C112Y mutant plasmid together with pDsRed-ER, pDsRed-Monomer-Golgi or pPM-mKeima-Red for 24 h. They were stained with anti-uromodulin and Alexa Fluor 488-conjugated secondary antibody (UMOD, *Green*). Shown are representative images obtained by a confocal microscope. *Bar* 50 μm. **e** Quantification of anti-uromodulin immunoreactivity. *Histogram* summarizing the ratios of Alexa 488/pDsRed-ER, pDsRed-Monomer-Golgi or pPM-mKeima-Red fluorescence ($n = 3$) $^{*}p < 0.05$

with anti-annexin V antibody indicated that the number of apoptotic cells was significantly higher in cells expressing the C112Y mutant in comparison with those expressing the WT (Fig. 3b). The number of Sub-G1 phase cells was also significantly higher in cells expressing the C112Y mutant than in cells expressing the WT (Fig. 3c).

Effects of xanthine oxidase inhibitor, topiroxostat, on apoptosis induced by the C112Y mutant

Since xanthine oxidase (XO) inhibitor is well known to reduce apoptosis, effects of XO. inhibitor topiroxostat on instability and apoptosis induced by C112Y mutant were examined. As shown in Supplementary Fig. 4, topiroxostat 30 μM increased the mature form of the C112Y mutant associated with an increase in its secreted form. Figure 4a shows effects of topiroxostat on the expression level of pro- and anti-apoptotic proteins. Topiroxostat significantly decreased the protein levels of p53, Bax, and cytochrome *c*, while it significantly increased the protein levels of Bcl-2 and Bcl-xl. As expected, topiroxostat significantly decreased Annexin-V positive cells (Fig. 4b).

Discussion

In the present study, we identified a novel mutation C112Y in *UMOD* in a Japanese patient with FJHN. The levels of the mature and immature forms of the mutant protein were remarkably reduced in transfected HEK293 cells in comparison with the WT. The C112Y mutant had a shorter half-life and a higher level of polyubiquitination, resulting in a decreased steady-state level of the protein, suggesting its instability and proteasomal degradation [2]. The C112Y

Fig. 2 continued

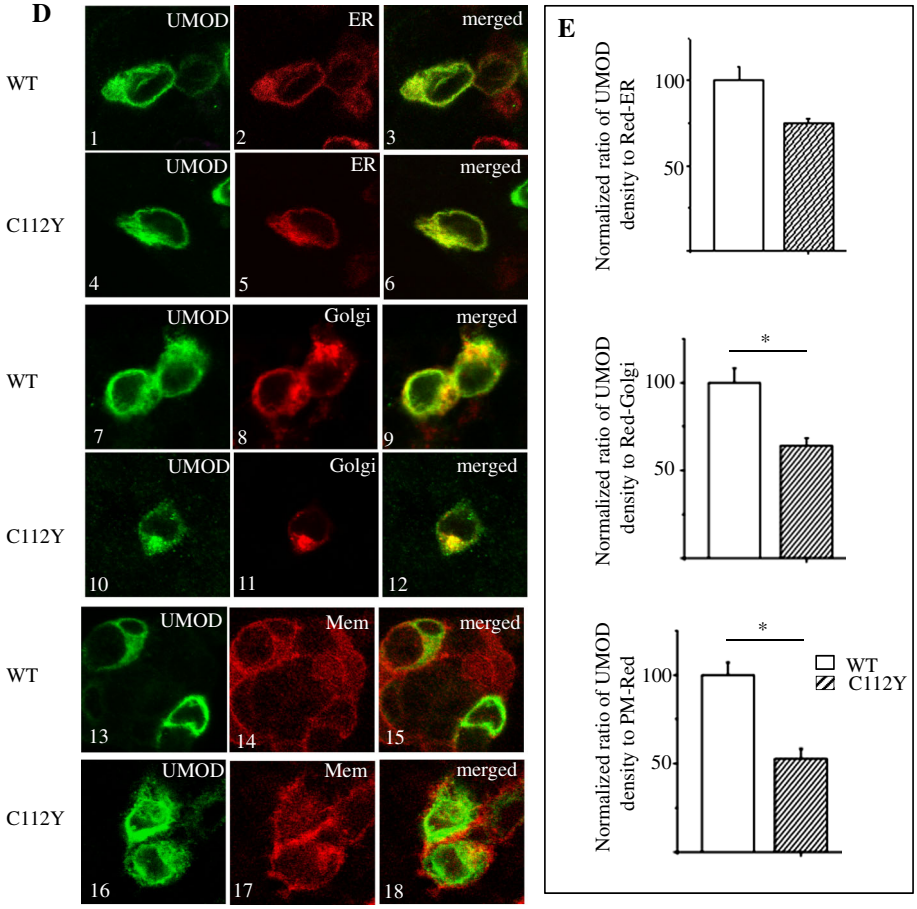

mutant was mainly distributed in the ER, and it was reduced in the Golgi apparatus and on the plasma membrane.

The mature form of C112Y was less abundant than that of WT, suggesting impaired maturation. The maturation of uromodulin from its 84 kDa precursor to 97 kDa glycosylated form depends on the retention time in the ER. The rate-limiting step is the formation of the correct sets of disulfide bonds in that component [13]. C112Y mutation is expected to inhibit the disulfide bond formation between C112 and C126 in the EGF-like domain [17]. A part of the C112Y mutant reached the cell membrane and was secreted into the culture medium. Similar secretion was observed for another mutant (C217G) [18].

Since the proper folding of uromodulin requires various factors such as protein-disulfide-isomerase, peptidyl-prolyl-*cis–trans*-isomerases, and molecular chaperones, C112Y might mature via these factors in the ER [19]. Proteasome inhibitors MG132 and lactacystine restored not only the cellular levels of the mature and immature forms of the C112Y mutant but also the levels of the secreted protein. These results indicated that UPS plays a pivotal role in degradation of the C112Y mutant and that inhibition of its degradation by proteasomal inhibitors prolonged the life-span of the C112Y mutant as well as the retention time of the C112Y in the ER to facilitate its interaction with molecular chaperons. Jennings et al. [20] reported that treatment with MG132 decreased the secreted N128S mutant uromodulin without changes in the cytosolic N128S, indicating the action of proteasomal inhibitors might be different among the mutations.

It is well known that misfolded proteins form aggregates through cross-linking via nonnative intrachain disulfide bonds [15] in the ER, causing cellular apoptosis [21]. We and other group previously reported that the instable mutant of cardiac myosin-binding protein C (MyBPC) (E334K) caused cardiac cellular apoptosis which was associated with increases of p53, Bax and cytochrome *c* and decreases of Bcl-2 and Bcl-xl [16]. In the present study, the expression of the C112Y mutant caused cellular apoptosis by increasing the levels of pro-apoptotic proteins and by decreasing the level of anti-apoptotic proteins. The findings observed for the C112Y mutant seem to be comparable with those for the cardiac MyBPC mutant.

The most prominent finding is the action of a XO inhibitor, topiroxostat, on apoptosis induced by C112Y.

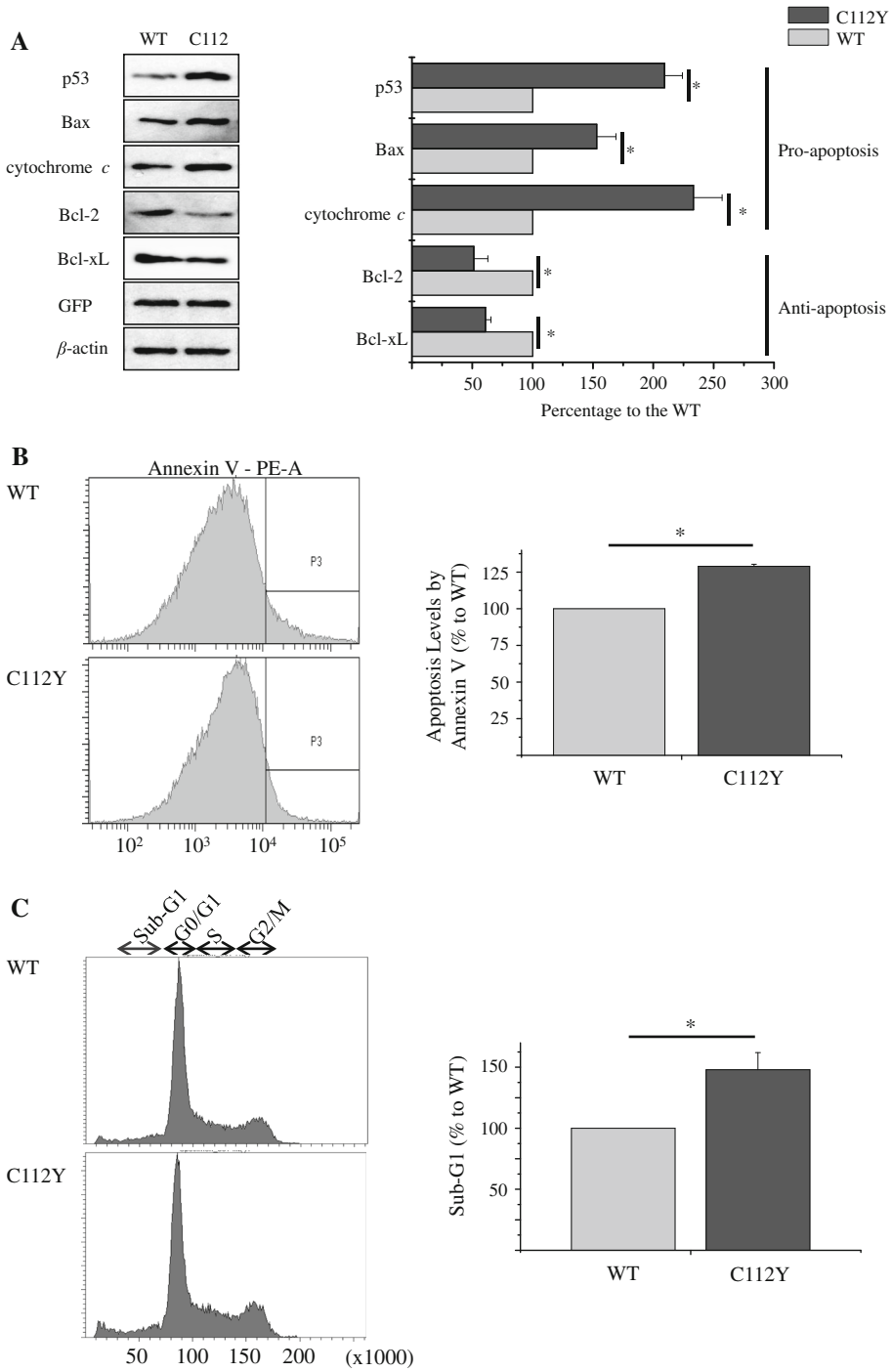

Fig. 3 Expression of pro- and anti-apoptotic proteins and cellular apoptosis. **a** The levels of pro- and anti-apoptotic proteins in HEK293 cells expressing WT or C112Y mutant for 72 h. *Left* representative Western blot with the indicated antibodies; *right* quantitative densitometric analysis of the indicated proteins ($n = 4$–6). *$p < 0.05$. **b** Flow cytometric analysis of the cell population stained with annexin V. Two hundred thousand cells expressing either WT or C112Y mutant for 72 h were analyzed by FACscan. *Left* the representative plot of annexin V-positive cells; *right* the % of annexin V-positive cells expressing C112Y mutant normalized to those in WT ($n = 3$). *$p < 0.05$. **c** FACS analysis of the cell population in the sub-G1 phase. *Left* the representative plot of cell population in each cell cycle phase; *right* the percentage of sub-G1 phase of cells expressing WT or C112Y mutant ($n = 3$). *$p < 0.05$. Data are shown as mean ± SEM, calculated by unpaired, two-tailed Student's *t* test

The accumulation of misfolding protein causes ER stress to produce the reactive oxidative species (ROS) in ER and mitochondria [22]. Mitochondrial dysfunction via extensive generation of ROS activates the mitochondria-dependent apoptotic machinery by directly triggering the release of the apoptogenic molecule cytochrome *c* from affected mitochondria in protein misfolding disease pathogenesis [23]. While ROS is reported to be produced via activation of either XO as well as NADPH oxidase, an authentic XO inhibitor oxypurinol has been reported to decrease ROS to protect mitochondrial dysfunction in the desmin-related myopathy, which supports the idea that reduction of ROS by XO inhibitor might reduce cytochrome *c* release from mitochondria, suppressing apoptosis. In the present study, topiroxostat, an XO inhibitor, reduced expression of pro-apoptotic protein cytochrome *c* in cells expressing C112Y

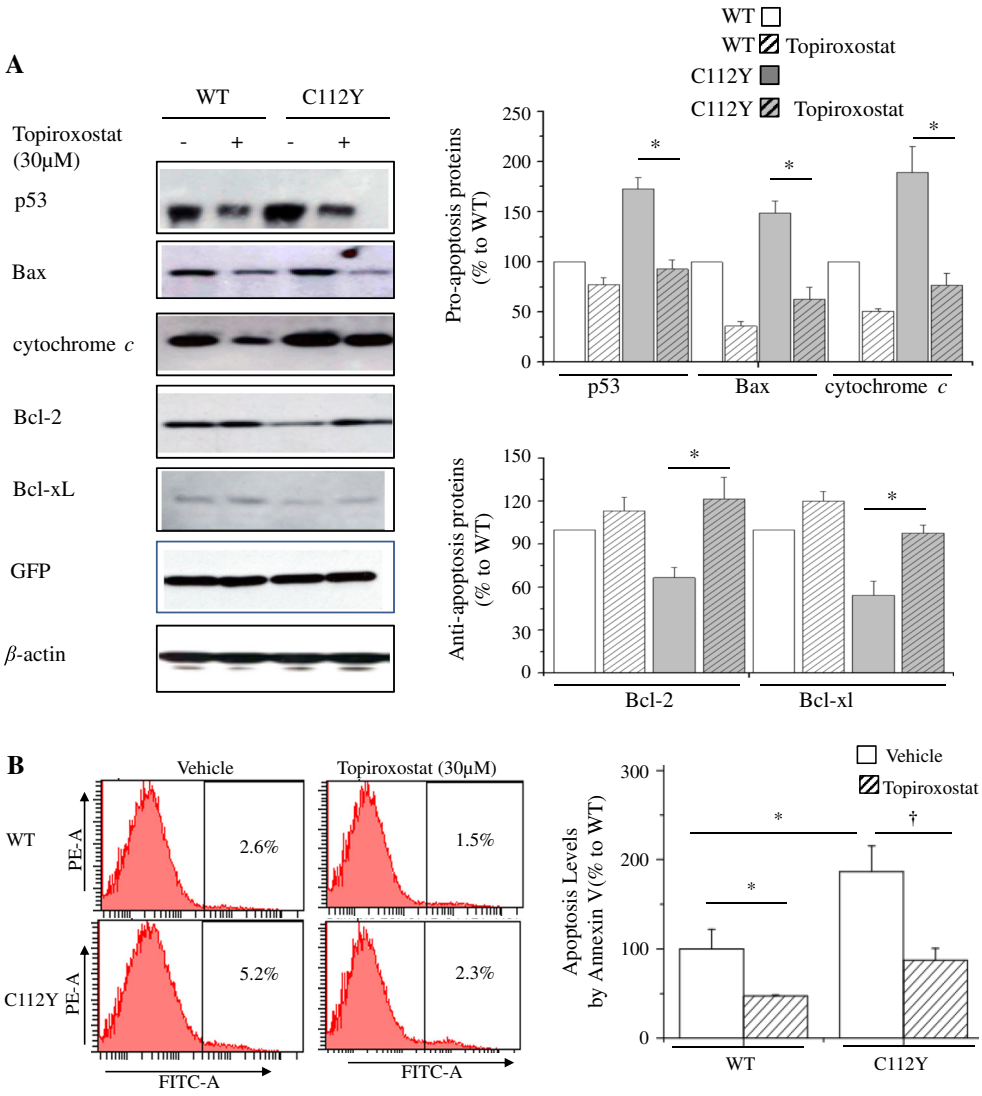

Fig. 4 Effects of topiroxostat on the pro- and anti-apoptotic proteins and apoptosis. **a** Protein levels of p53, Bax, cytochrome *c*, Bcl-2, and Bcl-xL with or without treatment of topiroxostat (30 μM, 24 h) in HEK293 cells expressing WT or C112Y mutant for 72 h. Shown are representative blots (*left*); quantitative densitometric analysis of the indicated proteins (*right*) ($n = 4$–6). $^{*}p < 0.05$. **b** Flow cytometric analysis of the cell population stained with annexin V. Two hundred thousand cells expressing either WT or C112Y mutant for 72 h with or without treatment of topiroxostat (30 μM) were analyzed by FACscan. *Left* the representative plot of annexin V-positive cells; *right* the % of annexin V-positive cells expressing C112Y mutant normalized to those in WT ($n = 3$) with or without topiroxostat. $^{*}p < 0.05$, $^{\dagger}p < 0.05$

and reduced apoptosis, indicating that topiroxostat inhibited the mitochondria-dependent apoptotic pathway. Choi et al. [11] reported that allopurinol failed to reduce apoptosis in cells expressing mutant uromodulin, whereas colchicine and sodium 4-phenylbutyrate were effective. Further study is necessary to clarify the different actions of topiroxostat and allopurinol.

Although the precise mechanism of action of topiroxostat is unclear, the clinical implication is obvious. Topiroxostat can be administered to patients with even moderate renal failure for treating hyperuricemia, since pharmacokinetics of neither unchanged topiroxostat nor of its metabolite is not affected by moderate renal dysfunction [24]. Recently, topiroxostat has been reported to reduce both the serum uric acid levels and the urinary albuminuria in chronic kidney disease at stage 3 with hyperuricemia [24]. Since the present study showed that topiroxostat could protect mutant uromodulin-induced cellular apoptosis, this agent can be applied to the patients with FJHN for not only controlling the serum uric acid level but also to attenuate their kidney damage.

Conflict of interest This study was partially supported by Sanwa Kagaku Kenkyusho Co., Ltd. and Fuji Yakuhin Co., Ltd.

References

1. Hart TC, Gorry MC, Hart PS, et al. Mutations of the UMOD gene are responsible for medullary cystic kidney disease 2 and familial juvenile hyperuricaemic nephropathy. J Med Genet. 2002;39:882–92.
2. Turner JJ, Stacey JM, Harding B, et al. Uromodulin mutations cause familial juvenile hyperuricemic nephropathy. J Clin Endocrinol Metab. 2003;88:1398–401.
3. Pennica D, Kohr WJ, Kuang WJ, et al. Identification of human uromodulin as the Tamm–Horsfall urinary glycoprotein. Science. 1987;236:83–8.

4. Cavallone D, Malagolini N, Serafini-Cessi F. Mechanism of release of urinary Tamm-Horsfall glycoprotein from the kidney GPI-anchored counterpart. Biochem Biophys Res Commun. 2001;280:110–4.
5. Bachmann S, Koeppen-Hagemann I, Kriz W. Ultrastructural localization of Tamm–Horsfall glycoprotein (THP) in rat kidney as revealed by protein A-gold immunocytochemistry. Histochemistry. 1985;83:531–8.
6. Bates JM, Raffi HM, Prasadan K, et al. Tamm–Horsfall protein knockout mice are more prone to urinary tract infection: rapid communication. Kidney Int. 2004;65:791–7.
7. Mo L, Huang HY, Zhu XH, et al. Tamm–Horsfall protein is a critical renal defense factor protecting against calcium oxalate crystal formation. Kidney Int. 2004;66:1159–66.
8. Yu CL, Tsai CY, Lin WM, et al. Tamm–Horsfall urinary glycoprotein enhances monokine release and augments lymphocyte proliferation. Immunopharmacology. 1993;26:249–58.
9. Saemann MD, Weichhart T, Zeyda M, et al. Tamm–Horsfall glycoprotein links innate immune cell activation with adaptive immunity via a Toll-like receptor-4-dependent mechanism. J Clin Invest. 2005;115:468–75.
10. Online Mendelian Inheritance in Man, OMIM. Johns Hopkins University, Baltimore, MD. MIM Number: {162000}:{8/26/2003}: {603860}: {7/29/2003}:{191845}:{4/25/2005}. http://www.ncbi.nlm.nih.gov/omim/. Accessed 5 Jan 2010.
11. Choi SW, Ryu OH, Choi SJ, et al. Mutant Tamm–Horsfall glycoprotein accumulation in endoplasmic reticulum induces apoptosis reversed by colchicine and sodium 4-phenylbutyrate. J Am Soc Nephrol. 2005;16:3006–14.
12. Williams SE, Reed AAC, Galvanovskis J, et al. Uromodulin mutations causing familial juvenile hyperuricaemic nephropathy lead to protein maturation defects and retention in the endoplasmic reticulum. Hum Mol Genet. 2009;18:2963–74.
13. Rampoldi L, Caridi G, Santon D, et al. Allelism of MCKD, FJHN and GCKD causedby impairment of uromodulinexport dynamics. Hum Mol Genet. 2003;12:3369–84.
14. Kumar S, Muchmore A. Tamm–Horsfall protein-uromodulin (1950–1990). Kidney Int. 1990;37:1395–401.
15. Hurtley SM, Helenius A. Protein oligomerization in the endoplasmic reticulum. Annu Rev Cell Biol. 1989;5:277–307.
16. Bahrudin U, Morisaki H, Morisaki T, et al. Ubiquitin–proteasome system impairment caused by a missense cardiac myosin-binding protein C mutation and associated with cardiac dysfunction in hypertrophic cardiomyopathy. J Mol Biol. 2008;384:896–907.
17. Branza-Nichita N, Lazar C, Durantel D, et al. Role of disulfide bond formation in the folding and assembly of the envelope glycoproteins of a pestivirus. Biochem Biophys Res Commun. 2002;296:470–6.
18. Ma L, Liu Y, El-Achkar TM, et al. Molecular and cellular effects of Tamm–Horsfall protein mutations and their rescue by chemical chaperones. J Bio Chem. 2012;287:1290–1305.
19. Li S, Yang Z, Gordon WC, et al. Secretory defect and cytotoxicity: the potential disease mechanisms for the retinitis pigmentosa (RP)-associated interphotoreceptor retinoid-binding protein (IRBP). J Bio Chem. 2013;288:11395–406.
20. Jennings P, Aydin S, Kotanko P, et al. Membrane targeting and secretion of mutant uromodulin in familiar juvenile hyperuricemic nephropathy. J Am Soc Nephrol. 2007;18:264–73.
21. Vylet'al P, Kublova M, Kalbacova M, et al. Alterations of uromodulin biology: a common denominator of the genetically heterogeneous FJHN/MCKD syndrome. Kidney Int. 2006;70:1155–1169.
22. Cao SS, Kaufman RJ. Endoplasmic reticulum stress and oxidative stress in cell fate decision and human disease. Antioxid Redox Signal. 2014;21:396–413.
23. Maloyan Al, Osinska H, Lammerding J, et al. Biochemical and mechanical dysfunction in a mouse model of desmin-related myopathy. Circ Res. 2009;104:1021–8.
24. Hosoya T, Ohno I, Nomura S, et al. Effects of topiroxostat on the serum urate levels and urinary albumin excretion in hyperuricemic stage 3 chronic kidney disease patients with or without gout. Clin Exp Nephrol. 2014 [Epub ahead of print].